Transactions on Additive Manufacturing Meets Medicine
Trans. AMMM, 2025, Vol. 7, No 1, Article ID 2076, 5 Pages

Infinite Science Publishing

Original Research Article

A 3D printed hand model of Bennett's and 5th metacarpal shaft fractures

T. Wright[1], S. Williams[1], J. Qiu[1*], B. Murphy[2,4], S. O. P. Hofer[3,4], and J. Catapano[2,4]

[1] *Techna, University Health Network, Toronto, Canada*
[2] *Unity Health Toronto, Toronto, Canada*
[3] *University Health Network, Toronto, Canada*
[4] *University of Toronto, Toronto, Canada*
[*] *Corresponding author, email: jimmy.qiu2@uhn.ca*

Abstract: Percutaneous fracture fixation of hand fractures using Kirschner wires is a difficult skill for learners to develop due to difficulties in spatial visualization, fracture alignment, fluoroscopic guidance, and instrument handling. Realistic models are required to improve surgical education and skill acquisition outside the operative setting. This study examines the utilization of 3D printing, silicone casting, and electromagnetic (EM) tracking to fabricate reproducible multi-material hand fracture models simulating Bennett's and 5th metacarpal shaft fractures. CT images of a healthy hand were segmented to create 3D reference meshes for bones and skin. Artificial fractures were introduced and the skin mesh updated to reflect displacements. Bone meshes were modified for 3D printing and EM integration by incorporating features such as fracture bridging, through-holes for silicone adhesion, wire channels for sensor placement, registration fiducials, and a baseplate for mold alignment.

I. Introduction

K-wire fixation is a minimally invasive method for treating hand fractures by stabilizing broken bones using thin steel Kirschner wires (K-wires). Correct fixation requires spatial knowledge and technique to align the broken bone fragments in order to restore anatomical geometry, proper alignment of K-wire entry and trajectory, the use of fluoroscopy for image-guidance, and insertion of the K-wire until final fixation is complete and verified with fluoroscopy.

The execution of K-wire fixation during surgical intervention can be challenging for new learners and residents due to limitations in spatial understanding, access to realistic models, and fluency with surgical instruments and fluoroscopy systems. Recent studies have demonstrated that 3D-printed models enhance skill acquisition in competency-based surgical education. These models are not only cost-effective but also provide realistic simulations that better prepare trainees for real-life operations [1-4].

Prior work by Prsic et al. [3] describes a take home 3D-printed hand model with bone 3D-printed in Acrylonitrile Butadiene Styrene (ABS) plastic and silicone skin soft tissue, allowing learners of different skill levels to practice with real K-wires both with and without fluoroscopy, using opaque or transparent silicone respectively. Papavasiliou et al. [4] describe a similar manufacturing process with the addition of elastic bands to mimic collateral ligaments and the assessment of various infill settings for their impact on radiopacity during fluoroscopy guidance. Ibbeken et al. [9] describes similar model development and manufacturing steps involving medical image segmentation, creation of a casting mold, silicone soft tissue casting, and use of computed tomography (CT) control scans to measure distances for accuracy and reproducibility assessments of an upper airway phantom.

This paper describes a process for manufacturing reproducible hand fracture models that integrate polyurethane foam with silicone soft tissue to more accurately mimic the compressive and tensile properties of soft tissue [5, 6] at the fracture site. CT of the 3D-printed models is used to assess the reproducibility of the manufacturing process relative to the reference CT scans. In addition, the manufacturing process incorporates electromagnetic (EM) sensors that enables 6-Degrees-of-

Freedom (DoF) motion tracking of non-fractured and fractured bones.

II. Material and methods

II.I Hand meshes

CT images of a healthy left hand from a patient was selected from the hospital's database at St. Michael's Hospital. Threshold-based segmentation was used to export Standard Tessellation Language (.STL) meshes of the bone and skin tissue using ITK-SNAP [7]. The threshold-based segmentation meshes were then imported into Blender (Blender Foundation, Amsterdam, NL) and Meshmixer (Autodesk Inc., San Francisco, CA, USA) for further post-processing, including the removal of non-manifold geometry and isolated islands, mesh smoothing, the addition of Bennett's and 5th metacarpal shaft fractures, and mesh modifications for additive manufacturing.

II.II Bennett's and 5th metacarpal shaft fractures

Bennett's and 5th metacarpal fractures were artificially introduced in the thumb and the 5th digit using Blender with resulting fracture breaks and geometry reviewed by expert surgeons. For the Bennett's fracture, a break was introduced in the bone mesh at the base of the thumb. For the 5th metacarpal shaft fracture, an oblique break was introduced at the shaft of the 5th digit. Skin meshes were then adjusted to match the new thumb and 5th digit positions (Fig. 1a-b).

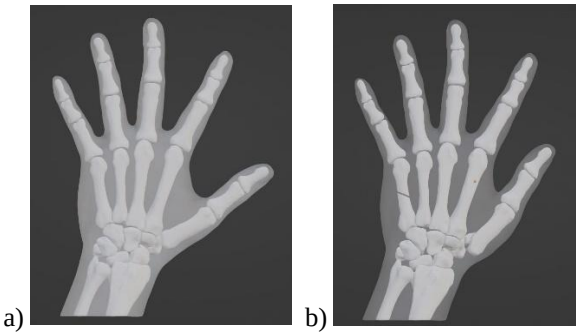

Figure 1: 3D models of the (a) reference left hand, (b) modifications for Bennet's and 5th metacarpal shaft fractures.

II.III Modifications for additive manufacturing and EM sensor integration

Autodesk Fusion 360 (Autodesk Inc, San Francisco, CA, USA) was used to modify the generated meshes from section II.II to prepare them for 3D printing and soft tissue casting including the addition of

- Fracture bridges at the Bennett's and 5th metacarpal shaft fracture sites, allowing the bone to be fabricated in a single print and broken once silicone soft tissue is cast (Fig. 2a-b).
- Divot points and wire channels for attachment of EM sensors, enabling co-registration with EM tracking for the hand, thumb, and 5th digit (Fig. 3a-e).
- Through-holes in the bone mesh to improve silicone adhesion (Fig. 4a-b). A two-part mold for silicone casting, including the addition of a base plate for the bone mesh to enable its suspension and correct spatial alignment during silicone casting.

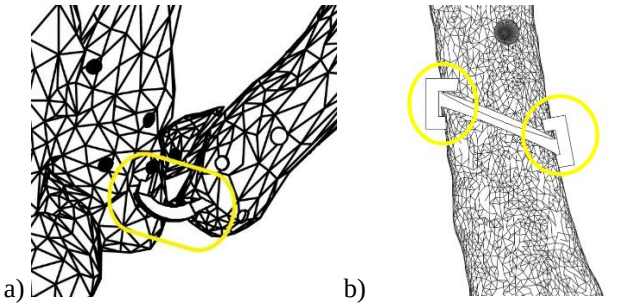

Figure 2: Modification of bridges at fracture sites for (a) the thumb, (b) 5th metacarpal shaft.

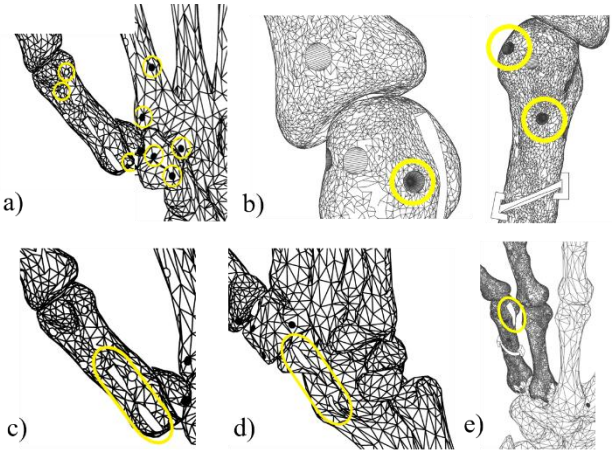

Figure 3: Fiducial points and wire channels for EM registration: (a) fiducial point on the hand and thumb, (b) fiducial points on the 5th metacarpal shaft above the oblique fracture, (c) wire channel on the thumb, (d) wire channel on the hand, (e) wire channel on the 5th metacarpal shaft.

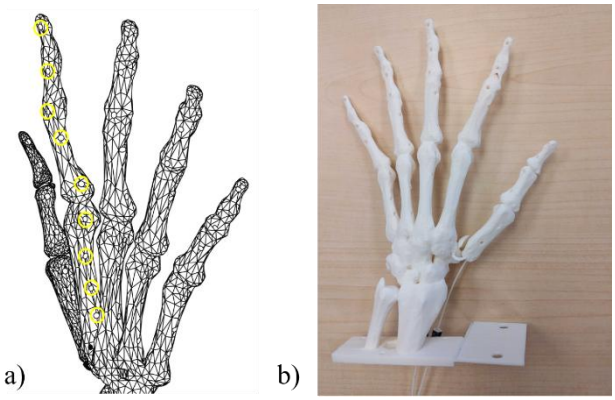

Figure 4: Addition of silicone adhesion through-holes (a) highlighted on the 4th metacarpal and phalanx, (b) across all metacarpals and phalanges 3D printed as full hand.

II.IV Additive manufacturing

The bone and two-part mold pieces were 3D printed using a Prusa i3 MK3S+ (Prusa Research, Prague, CZ) with a layer height of 0.15 mm and an XY tolerance of 0.3 mm to print components in polylactic acid (PLA) plastic. Northern Digital Inc. (NDI) Aurora (Waterloo, ON, CA) 6-DoF EM sensors were positioned and secured in wire channels with hot-melt adhesive before rigid registration was completed using a tracked stylus and fiducial divot points on the bone model.

Smooth-On (Smooth-On Inc., Macungie, PA, USA) FlexFoam-iT polyurethane foam was poured onto the Bennett's and 5th metacarpal shaft fracture sites ensuring encapsulation (Fig. 5a). After polyurethane application and curing, the hand was secured into the mold, followed by silicone soft tissue casting using Smooth-On EcoFlex 00-30.

After silicone curing, the hand was removed from the two-part mold, the excess silicone trimmed from seam lines of the two-part mold, and the fracture bridges were broken at the Bennett's and 5th metacarpal shaft fracture sites to enable independent freedom of motion of the non-fractured and fractured segments (Fig. 5b-c).

A flowchart of model development and manufacturing is included to summarize steps (Fig. 6).

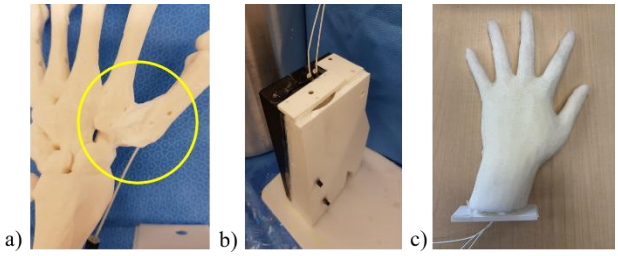

Figure 5: Mold and casting of the hand with Bennett's and 5th metacarpal shaft fractures: (a) Smooth-On FlexFoam-iT poured and set at the Bennett's fracture site, (b) bone model aligned with two-part mold, (c) resulting cured model of the hand.

II.V Reproducibility testing

The evaluation of 3D printing reproducibility with the Prusa i3 MK3S+ was performed with four 3D printed partial thumb and index sets based on the reference CT described in section II.I. A Siemens Cios Spin conebeam CT was used to scan the 3D prints at 0.5 mm voxel resolution. MeshLab (ISTI – CNR, Pisa, IT) was then used to align the resulting cone-beam CT segmentation meshes with the reference CT meshes to assess 3D printing errors using the Hausdorff distance, calculated as the mean of the point-to-point distances between corresponding vertices of a partial set and the reference CT. The final error is reported as the mean of the four average Hausdorff distances.

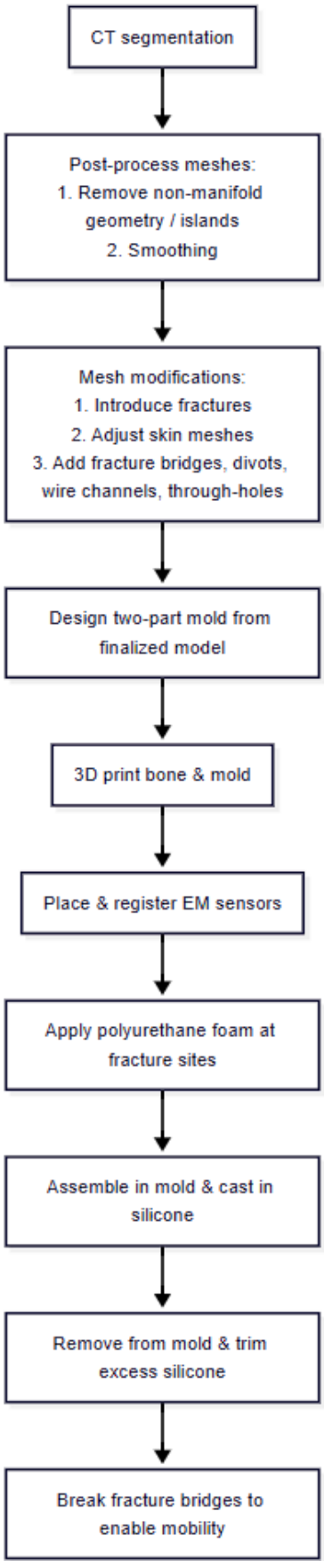

Figure 6: Flowchart summary of model development and manufacturing steps.

Three iterations of full hands were fabricated with EM sensors to calculate corresponding fiducial registration errors (FREs) between the 3D printed hand, thumb, 5th digit and their corresponding 3D meshes, where recorded positions of fiducial divots using a calibrated EM stylus were used for rigid registration of the hand, the thumb, and the 5th digit respectively. After registration, the target registration errors (TREs) were estimated using Fitzpatrick's method [8] to predict how errors propagate to other mesh points with respect to the FRE (Fig. 7a-c).

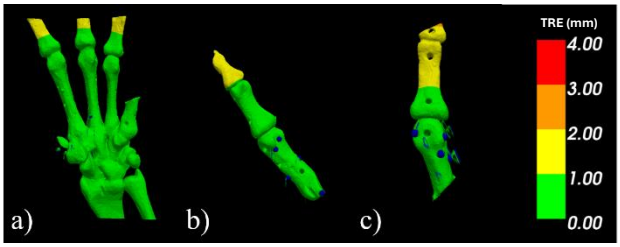

Figure 7: Visualizations of TREs after rigid registration of the (a) hand, (b) thumb, and (c) 5th metacarpal shaft.

II.VI Range of motion measurements

Range of motion assessments were performed with respect to the resting position and orientation of the thumb and 5th metacarpal bones. The proximal-distal axis (Y-axis) was defined as the line extending from the base to the tip of the finger in its resting position; the radial-ulnar axis (X-axis) was defined by the line connecting the radial and ulnar sides of the phalanx; and the dorsal-volar axis (Z-axis) was determined by the cross product of the proximal-distal and radial-ulnar axes. The origin of the principal axes was set to be the base of the 2nd phalanx of the thumb and the 5th metacarpal shaft above the oblique fracture in their corresponding resting positions.

Translational ranges were measured along the proximal-distal axis for compression and expansion ranges. Angle ranges were calculated by rotating the fractured bones in the planes defined by the principal axes. Specifically, the X-axis angle was computed from rotations in the Y–Z plane, the Y-axis angle from rotations in the X–Z plane, and the Z-axis angle from rotations in the X–Y plane.

III. Results and discussion

The material cost for the hand model totals CA $1,930.17, with $1,890.00 allocated to the three EM sensors. Fabrication requires 1.83 labor hours, encompassing processing of bones, EM attachment and registration, as well as preparing, casting, and post-processing the mold and model. Additionally, 79.2 passive hours are required for printing and curing. The total time includes 27 hours to print each side of the mold and 16.75 hours to print the bones on a single printer, along with almost 5 hours of curing time.

The average Hausdorff distance values were 0.11 mm and 0.12 mm for the index and thumb after mesh alignment with respect to the reference CT (Table 1). The average fiducial registration errors across three hands were 0.55 mm, 0.69 mm, and 0.74 mm for the hand, thumb, and 5th digit respectively (Table 2). TREs across mesh points were below 1.0 mm around fracture sites for the hand, thumb, and 5th metacarpal shaft.

Table 1: Hausdorff distance between 3D printed partial sets and reference CT mesh.

Partial Set	**Average Hausdorff Distance (mm)**	
	Index	**Thumb**
1	0.11	0.12
2	0.09	0.11
3	0.12	0.12
4	0.13	0.14
Overall Average	0.11	0.12

For the thumb, translational motion along the proximal-distal axis ranged from 5.5 mm of compression to 12.43 mm of extension. X-axis angles ranged between 62.87 degrees and (towards volar) 38.37 degrees (towards dorsal), Y-axis angles ranged between 28.36 degrees (towards volar) and 61.25 degrees (towards dorsal), and Z-axis angles ranged between 56.98 degrees (towards radial) and 19.01 degrees (towards ulnar).

With the 5th metacarpal shaft, translational motion along the proximal-distal axis ranged from 2.66 mm of compression to 10.33 mm of extension. X-axis angles ranged between 67.25 degrees (towards volar) and 55.57 degrees (towards dorsal), Y-axis angles ranged between 31.36 degrees (towards volar) and 39.46 degrees (towards dorsal), and Z-axis angles ranged between 14.11 degrees (towards radial) and 51.59 degrees (towards ulnar).

Table 2: TREs of fabricated hands.

Hand Set	**Fiducial Registration Error (mm)**		
	Hand	**Thumb**	**5th Digit**
1	0.63	0.65	0.70
2	0.24	0.68	0.74
3	0.78	0.73	0.77
Overall Average	0.55	0.69	0.74

The majority of the model's material cost (98%) is driven by the three EM sensors (CA $630 each) required to co-register motion at the thumb and 5th metacarpal fracture sites relative to the hand. Although these sensors represent a significant cost, the use of EM tracking enables virtual scenarios for virtual x-rays and K-wire placement exercises on the same physical model, which is not possible with traditional static simulators.

The sub-millimeter Hausdorff distances (<0.13 mm) and fiducial registration errors (<0.75 mm) demonstrate high reproducibility in spatial accuracy and sensor registration across multiple prints.

The addition of silicone through-holes and polyurethan foam enables mobility around fracture sites, allowing proper reduction setting. To enhance clinical and training utility, future work will integrate the use of real-time EM tracking with virtual x-rays and guided K-wire placements, supporting quantitative, repeatable learner assessments of fracture reduction and K-wire placement accuracy.

IV. Conclusions

This work describes a reproducible pipeline for creating hand fracture models with rigid bone and flexible silicone soft tissue. The incorporation of polyurethane foam at fracture sites enables realistic compressive and tensile properties around the fracture site.

The integration and use of EM sensors allow 6-DoF motion tracking of the non-fractured and fractured bones in the fabricated models, enabling quantitative assessment of spatial positioning, orientation, and alignment.

While this paper focuses on the fabrication of 3D printed hand fracture models integrated with EM sensors, future work will leverage the use of EM sensors and full 6-DoF tracking for spatially guided teaching and feedback.

Although the EM sensors lead to a higher production cost, the integration of motion data will enable quantitative spatial evaluation and visualization for learners. These extensions include the use of virtual x-rays, evaluation of fracture reductions, and placements of virtual K-wires.

Acknowledgments

Research funding: The authors state no funding involved.

Author's statement

Authors state no conflict of interest.

References

[1] Y. Jiang, H. Jiang, Z. Yang, Y. Li, The current application of 3D printing simulator in surgical training, Frontiers in Medicine, vol. 11, 1443024, Aug. 2024.

[2] A. Hecker, L. Tax, B. Giese, M. Schellnegger, A. L. Pignet, P. Reinbacher, N. Watzinger, L. P. Kamolz, D. B. Lumenta, Clinical Applications of Three-Dimensional Printing in Upper Extremity Surgery: A Systematic Review, Journal of Personalized Medicine, vol. 13-2, 294, Feb. 2023.

[3] A. Prsic, M. K. Boyajian, W. K. Snapp, J. Crozier, A. S. Woo, A 3-dimensional-printed hand model for home-based acquisition of fracture fixation skills without fluoroscopy, Journal of Surgical Education, vol. 77-6, pp. 1341–1344, Nov. 2020.

[4] T. Papavasiliou, S. Chatzimichail, J. C. Chan, C. J. Bain, L. Uppal, A standardized hand fracture fixation training framework using novel 3D printed ex vivo hand models: our experience as a unit, Plastic and Reconstructive Surgery–Global Open, vol. 9, e3406, Feb. 2021.

[5] W. Clifton, A. Damon, F. Valero-Moreno, E. Nottmeier, M. Pichelmann, The SpineBox: a freely available, open-access, 3D-printed simulator design for lumbar pedicle screw placement, Cureus, vol. 12-4, Apr. 2020.

[6] K. Zerdzicki, A. Znaczko, A. Kondrusik, W. Korbut, Compressive and tensile properties of polyurethane foam mimicking trabecular tissue in artificial femoral head bones, Frontiers in Bioengineering and Biotechnology, vol. 12, 1482165, Jan. 2025.

[7] P. A. Yushkevich, J. Piven, H. C. Hazlett, R. G. Smith, S. Ho, J. C. Gee, G. Gerig, User-guided 3D active contour segmentation of anatomical structures: Significantly improved efficiency and reliability, Neuroimage, vol. 31-3, pp. 1116–1128, Jul. 2006.

[8] J. M. Fitzpatrick, J. B. West, C. R. Maurer, Predicting error in rigid-body point-based registration, IEEE Transactions on Medical Imaging, vol. 17-5, pp. 694–702, Oct. 1998.

[9] A. Ibbeken, C. Hagen, F. Zell, A. Steffen, U. Grzyska, A. Frydrychowicz, T. M. Buzug, Design and construction of a flexible pharyngeal phantom, Transactions on Additive Manufacturing Meets Medicine, vol. 3-1, 499, 2021.